Cadmium(II) Capture Using Amino Functionalized Hydrogel with Double Network Interpenetrating Structure: Adsorption Behavior Study

Sihua Liu
Hunan University of Technology
Haifei Wang
Hunan University of Technology
Jue Hu
Hunan University of Technology
Yue Li
Hunan University of Technology
guiyin zhou (gyzhou@hut.edu.cn)
Hunan University of Technology https://orcid.org/0000-0002-6913-0909

Research Article

Keywords: hydrogel, cadmium ion, adsorption behavior

Posted Date: May 19th, 2021

DOI: https://doi.org/10.21203/rs.3.rs-531371/v1

Cadmium(II) Capture Using Amino Functionalized Hydrogel with Double Network Interpenetrating Structure: Adsorption Behavior Study

Sihua liu[a,1], Haifei Wang[a,1], Jue Hu[a], Yue Li[b], Guiyin Zhou[a,*]

[a] College of Life Science and Chemistry, Hunan University of Technology, Zhuzhou, 412007, PR China

[b] School of Materials and Chemical Engineering, Henan University of Engineering, Zhengzhou, 450007, PR China

[1] The authors contributed equally to this work

[*] Correspongding author

E-mail: gyzhou@hut.edu.cn

Abstract: Heavy metal pollution caused by the indiscriminate disposal of toxic heavy metal wastewater has become one of the serious water environmental issues. In this study, a novel NH_2-PAA/Alginate hydrogel with double network interpenetrating structure was constructed with alginate, acrylic acid, and other raw materials. Characterized by SEM, this hydrogel shows a three-dimensional porous structure, which would be useful in adsorption process for its high diffusion coefficient. The results of adsorption experimental show that the NH_2-PAA/Alginate possessed the well adsorption capacity when pH above 3.5, the maximum adsorption capacity calculated by Langmuir was 176.5 mg/g, the adsorption equilibrium can be achieved within 150 min. In addition, the NH_2-PAA/Alginate has good recycling ability and stability. The results of XPS analysis reveal that the Cd(II) exchanged with Ca(II) and then coordinated with amino and hydroxyl groups in NH_2-PAA/Alginate. The NH_2-PAA/Alginate hydrogel can deal with all kinds of heavy metal ions and is a potential material for heavy metal adsorption.

Key words: hydrogel; cadmium ion; adsorption behavior.

1 Introduction

Water plays a vital role in the development of human society. While the increasing worldwide contamination of water systems has become one of the key environmental facing humanity [1]. According to “The Analysis Report of China's Industrial Effluent Treatment in 2019”, the industrial wastewater discharge accounts for 23.55% of the total wastewater discharge in China in 2017, which is 18.16 billion tons. The non-degradable and toxic heavy metal ions from the industrial effluent, such as cadmium ion, can accumulate in the body along with the biological chain, causing a serious of damage to human health. For example, damage central nervous system, liver and kidneys [2]. Therefore, the removal of such toxic metal ions from industrial effluent is becoming a crucial issue. Various treatment technologies, such as chemical precipitation [3], solvent extraction, reverse osmosis [4], ion-exchange [5], filtration [6], electrodialysis [7], have been employed to remove heavy metal ions from industrial effluent. While adsorption technology is regarded as one of the most promising technologies owning to its low cost and easy operate.

Still, there are many problems in practical application of adsorbent. For example, the granular adsorption such as activated carbon and chelating resin, have a large number of micropores and mesopores due to their high specific surface area [8], the slow internal diffusion rates of these adsorbents dominated by Knudsen diffusion seriously limit their overall kinetics and the equilibrium times commonly require some hours [9]. In addition, the granular materials are easily subject to blocking and burial of adsorption sites, resulting in partial loss of adsorption performance [10]. Although the nano-adsorbent possess the high surface energy which can accelerate the adsorption process [11], the difficult to separate for the nanoscale could result in the increase of operation cost and secondary pollution of the environment [12]. Magnetic nano-adsorbents solve the problem of nano material recovery [13], while the magnetic particles such as iron, cobalt, nickel particles are easy to fall off from the nano-adsorbent in the adsorption process [14]. Additionally, the inefficient regeneration of magnetic nano-adsorbents under acidic conditions greatly limits their practical

applications [15]. Therefore, it is of great significance to find a kind of adsorption material with high adsorption performance, easy separation and regeneration.

Polymer hydrogel is a material with characteristics of solid and liquid [16]. The diffusion coefficient of molecules in three-dimensional networks of hydrogel is close to that of water [17], although they possess macroscopical geometric structure. Sun group reported an extremely stretchable and tough dual network (DN) hydrogels by combining weak and strong crosslinks in 2012 [18]. The combination of relatively high stiffness, high toughness and recoverability of stiffness and toughness, along with an easy method of synthesis, make these materials ideal candidates for further investigation. Therefore, double network hydrogel has attracted much attention in many fields such as drug delivery [19], tissue engineering [20], environmental remediation [21].

In this study, a novel amino-group functionalized NH_2-PAA/Alginate DN hydrogel adsorption was designed and prepared using simple free-radical polymerization and modification. The physico-chemical properties of NH_2-PAA/Alginate hydrogel were characterized using SEM, FTIR and XPS analyses. The influence of initial pH of the solution, ionic strength, adsorbate concentration, adsorption time and temperature on NH_2-PAA/Alginate hydrogel were studied, and the adsorption performance of NH_2-PAA/Alginate hydrogel for Cd(II) was also evaluated. Furthermore, the adsorption mechanism was also discussed in detail.

2 Experimental part

2.1 Materials

Sodium alginate (viscosity 200 ± 20 mPa.s) was purchased from Tianjin Guangfu Fine Chemical Research Institute; Acrylic acid (analysis pure) was purchased from Shandong Qilu pharmaceuticals company and distilled under reduced pressure before use. Ammonium persulfate and triethylenetetramine were analytically pure and purchased from Sinopharm Chemical Reagent Co., Ltd; N,N-Methylenebisacrylamide, sodium bisulfite, calcium chloride, epichlorohydrin, analytically pure, purchased from

Shandong West Asia Chemical Industry Co., Ltd and used as received. All aqueous solutions were prepared with deionized water.

2.2 Preparation of hydrogel

NH_2-PAA/Alginate hydrogel was prepared using radical copolymerization and surface functional modification. As depicted in Fig. 1, 1.2 g acrylic acid and 0.3 g sodium alginate were added to 6 ml deionized water under stirring. Then the mixed solution, 0.025 g ammonium persulfate (initiator), 0.020 g sodium bisulfite (redox initiation system) and 0.025 g N,N-Methylenebisacrylamide (cross-linking agent) were added into a glass reactor. After ultrasonic under nitrogen atmosphere, the sealed reactor was placed in a water bath at 40℃ for 2 h to complete gelation process. The synthesized hydrogel was freeze-dried for 24 h and immersed in 5 wt% $CaCl_2$ solution for 2 h to cross-link the alginate network and got the PAA/Alginate hydrogel.

Next, after an immersion into 6 mL of dimethyl sulfoxide solution containing 0.1 g NaOH and 0.4 mL epichlorohydrin for 1 h at 60℃, the PAA/Alginate was further immersed into 6 mL of deionized water containing sodium hydroxide (20 wt%) and triethylenetetramine (0.6 mL) for 6 h at 60℃ to obtain NH_2-PAA/Alginate, which was washed with deionized water to remove unreacted reagents.

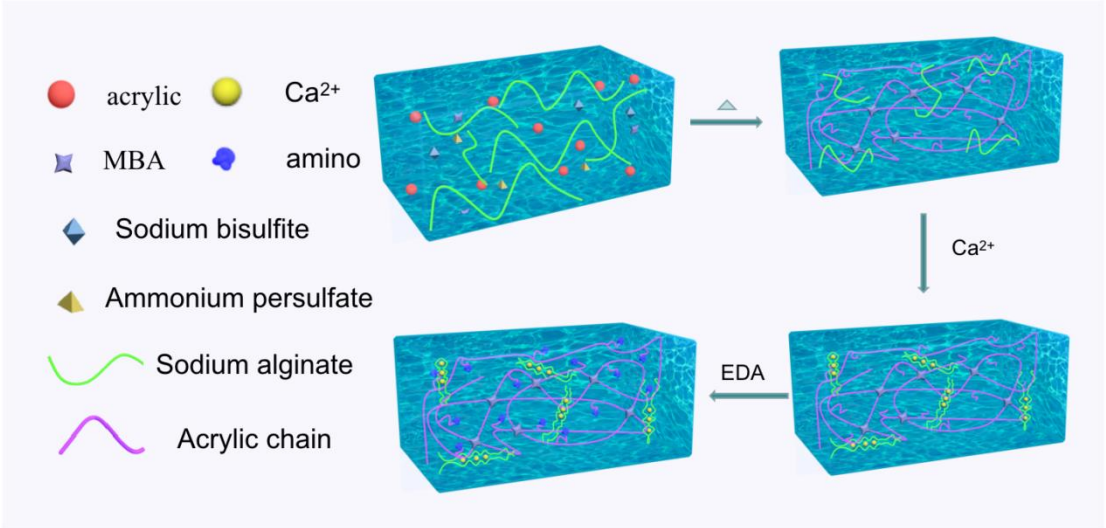

Fig. 1 Mechanisms of converting the composite into NH_2-PAA/Alginate DN hydrogels.

2.3 Characterization

The chemical structure of the samples was analyzed by Fourier transform infrared spectroscopy (FTIR, Nicolet 5700, Thermo Electron Scientific Instruments Corp. American). After the sample was ground into power with KBr and pressed into pellet, the test was analyzed in the range of 4000~500 cm^{-1}. The morphological features of freeze-dried NH_2-PAA/Alginate examined by scanning electron microscope (SEM, MIRA3, Tescan Ltd., Czech Republic). The thermal stability of NH_2-PAA/Alginate xerogel was analyzed by thermogravimetric analysis (TGA, TG/DTA7300, Hitachi, Ltd., Japan) from room temperature to 600℃ under a nitrogen atmosphere at a heating rate of 10℃/min. The surface chemistry of NH_2-PAA/Alginate before and after adsorbing Cd(II) was determined by X-ray photoelectron spectroscope (ESCALAB 250XI, Thermo Electron Scientific Instruments Corp. American). The compression experiment was implemented by electronic universal material testing machine (AG-Xplus, Shimadzu Ltd., Japan) with compression rate of 2mm/min. The zero charge point of the hydrogels was measured by ΔpH drift method. The 1 wt% xerogels were added into a series of solution with different pH and 0.01M NaCl. After 12 h at 25℃, the pH of the solution was measured again, and the intersection of curve with X axis of ΔpH *vs*. pH was the zero charge point of NH_2-PAA/Alginate. The swelling experiment was performed by immersing the hydrogels in an excess of water to reach swelling equilibrium at 25℃.

2.4 Batch adsorption experiments

The batch adsorption experiments were conducted using 1g/L NH_2-PAA/Alginate dry gel. Analytical grade $Cd(NO_3)_2$ were employed to prepare the Cd(II) stock solutions. The pH values of solution were adjusted by dilute HCl or NaOH solutions. NaCl, $MgCl_2$ or $CaCl_2$ were added as background electrolyte. After the suspensions were shaken under 160 rpm for 4 h, the concentrations of residuary Cd(II) in supernatant were measured by an atomic absorption spectrometer (AAS, AA-7020, Beijing Dongxi Analytical Instrument Co., Ltd., China). For the selectivity experiment, the mixed solution contains Cu(II), Cd(II), Pb(II), Zn(II), Mn(II) and Ni(II) ions, and the each ion concentration was 50 mg/L, the pH of the solution kept 5.0±0.1. For the regeneration

study, the Cd-NH_2-PAA/Alginate was eluted with 0.1M HCl solution, then regenerated with 0.1M NaOH solution, and washed with deionized water to neutral. The detailed experimental conditions were listed in the captions of figures for different experiments.

2.5 Data analysis

All the adsorption experiments were repeated twice. The equilibrium adsorption capacity q_e (mg·g^{-1}), adsorption efficiency E (%), distribution adsorption coefficient K_d (L·g^{-1}), and the swelling rate (SR) were calculated according to the following formula:

$$q_e=V(C_0-C_e)/m \quad (1)$$

$$E=(C_0-C_e)/C_0\times100\% \quad (2)$$

$$K_d=q_e/C_e \quad (3)$$

$$SR=(W_t-W_d)/W_t\times100\% \quad (4)$$

where V is the volume of the solution, m is the weight of the dry NH_2-PAA/Alginate, C_0 and C_e are the initial and equilibrium concentrations of Cd(II) ions. The W_t represents the mass of gel in swollen state at time t, and W_d is the mass of NH_2-PAA/Alginate xerogel.

2.6 Model Fitting

Kinetic models including pseudo-first-order, pseudo-second-order model and intraparticle diffusion model were employed to fit the experimental data, and the mathematical equations were expressed as follow:

$$q_t = q_e\left(1-\exp\left(-k_1 t\right)\right) \quad (5)$$

$$q_t = q_e\left(1-\frac{1}{1+q_e k_2 t}\right) \quad (6)$$

$$q_t = k_p t^{0.5} \quad (7)$$

where q_t (mg·g^{-1}) is adsorption capacity at t (min), k_1 (L·min^{-1}), k_2 (g·(mg·min)$^{-1}$) and

k_p (min^{-1}) are the corresponding adsorption rate constants.

Isothermal adsorption model including Langmuir, Freundlich, and Temkin model were used to fit the adsorption isotherms. The correlation coefficients (R^2) were used for comparing the model applicability. The parameters of isothermal adsorption were calculated by the following equations:

$$q_e = \frac{q_{\max} \cdot K_L \cdot C_e}{1 + K_L \cdot C_e} \tag{9}$$

$$q_e = K_F C_e^{1/n_F} \tag{10}$$

$$q_e = (RT / b_T) \ln A_T + (RT / b_T) \ln C_e \tag{11}$$

$$q_e = \frac{K_{LF} C_e^{1/n}}{1 + a_{LF} C_e^{1/n}} \tag{12}$$

where q_{max} ($mg \cdot g^{-1}$) is the maximum adsorption, K_L ($L \cdot mg^{-1}$), K_F ($L \cdot mg^{-1}$) and K_{LF} ($L \cdot mg^{-1}$) are the isotherm adsorption constant, respectively, n_F is the adsorption intensity, the A_T ($L \cdot g^{-1}$) is the Temkin isotherm equilibrium binding constant and b_T ($J \cdot mol^{-1}$) is the constant related to heat of sorption.

3 Results and discussion

3.1. Characterization of hydrogel

The freeze-dried NH_2-PAA/Alginate aerogel was used to characterize the internal structure of SEM, and the result is shown in Fig. 2a. As shown by SEM image, the NH_2-PAA/Alginate exhibited a three-dimensional porous structure, and such a morphological feature would improve the exposure of the adsorption sites and the diffusion of metal ions [22]. The bulk NH_2-PAA/Alginate (inset image in Fig. 2a) could be cut into different shape in need as well as easy separation. The compressive test of NH_2-PAA/Alginate was investigated with gradually increasing strain (ε) (Fig. 2b). It can be seen that the NH_2-PAA/Alginate achieved a compression stress of 724 Kpa when

the load deformation was 36%. After the immediate second cycle, the compression stress was up to 1.3 Mpa at ε=51%, meanwhile, the compression stress of second test is not as high as that of first, illustrating that the hysteresis was caused by unzipping the network of ionic cross-links [23]. Significantly, the guluronic acid in alginate chains can form ionic crosslinks through Ca(II), and the electrostatic interaction may enable synergistic energy dissipation [24].

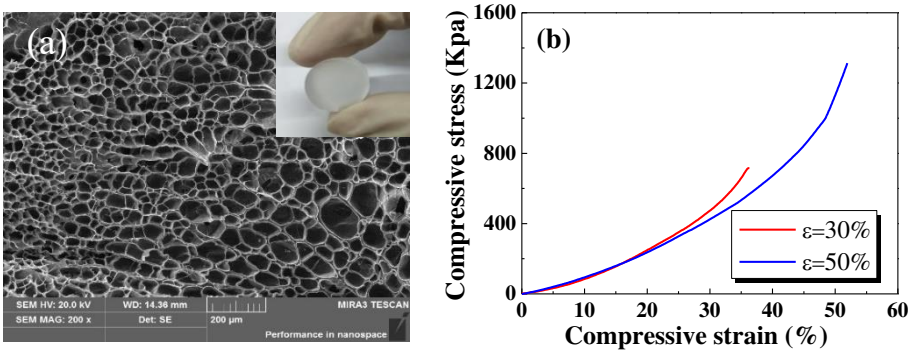

Fig. 2 (a) The SEM image of NH_2-PAA/Alginate. (b) Typical consecutive loading curves with gradually increased strain on NH_2-PAA/Alginate.

The group structure of the sample was analyzed by FTIR. As shown in Fig. 3a, the following functional groups were identified in PAA/Alginate: O-H, N-H stretching vibrations (3420 cm^{-1}), C-H stretching vibrations (2930 cm^{-1}), C=O stretching vibration (1670 cm^{-1}), C-O stretching vibrations (1300~1100 cm^{-1}) [25]. Compared with that of PAA/Alginate, two broader adsorptions appeared in NH_2-PAA/Alginate at 3180 and 1410 cm^{-1}, which corresponded to the stretching and bending vibration of amino N-H, respectively [26]. The FTIR spectra proved the existence of carboxyl and amino groups in NH_2-PAA/Alginate. The XPS results of NH_2-PAA/Alginate also confirmed the existence of oxygen- and amino-containing functional groups, a quantitative amount of the elements was determined by XPS element analysis and the results of the atomic content are listed in Table 1.

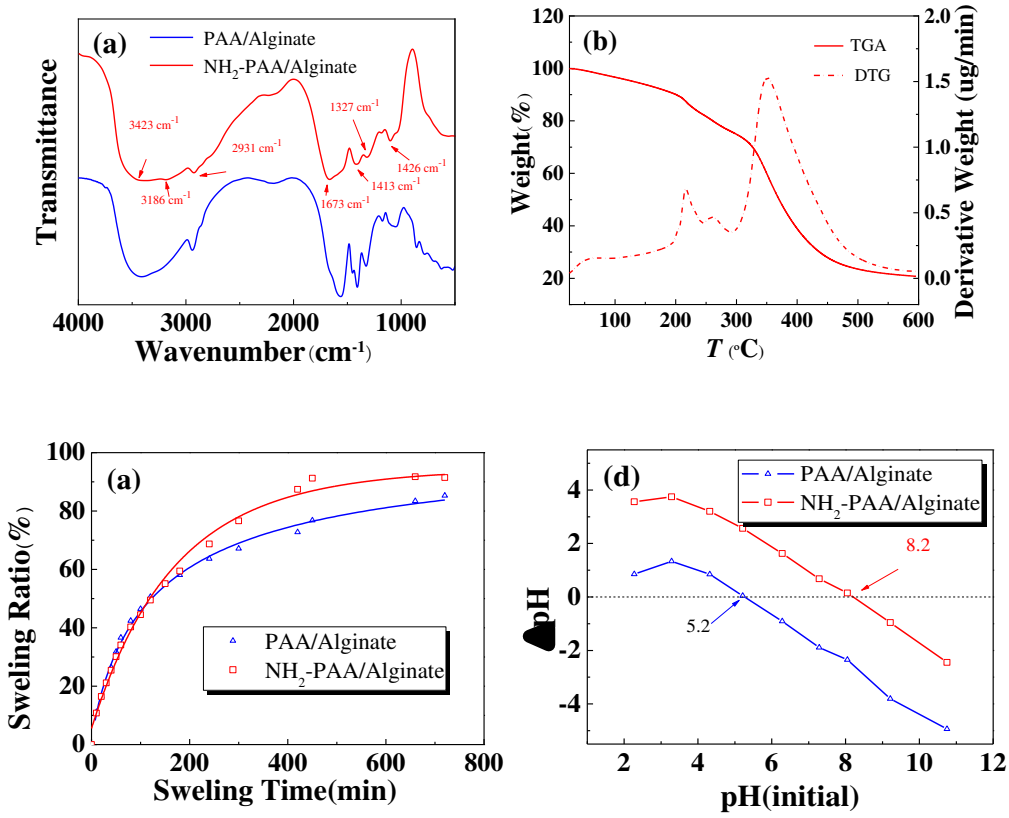

Fig. 3 (a) The FTIR spectra. (b) The TGA and DTG curves. (c) The swelling curves. (d) The pH_{pzc} measure of the hydrogel by ΔpH method.

Table 1 XPS analysis of element in the NH_2-PAA/Alginate

Name	NH_2-PAA/Alginate		Cd(II)- NH_2-PAA/Alginate	
	Atomic %	PP At. %	Atomic %	PP At. %
C1s	63.95	61.23	59.58	54.03
O1s	20.43	20.66	26.53	29.05
N1s	15.62	18.11	12.03	16.3
Ca	1.6	0.5	0.7	0.11
Cd	-	-	1.16	0.51

Fig. 3b shows the integral results from the thermogravimetric analysis (TGA) and the differential thermogravimetric data (DTG) analysis of NH_2-PAA/Alginate. The peak in DTG curve represents the temperature where the degradation rate is maximum for degradation stage in the whole process [27]. It can be seen that there are two

pyrolysis stages of the NH_2-PAA/Alginate, the first thermal degradation process occurred in the temperature range 200~300℃, which is attributed to the degradation of the amino, carboxyl and hydroxyl groups, as volatile gases were released [28]. The second stage occurred in the range 300~450℃, and is attributed to the depolymerization of polymer and formation of a carbonaceous residue.

The swelling behavior of hydrogels is shown in Fig. 3c. It can be seen that the SR of PAA/Alginate was about 85% at equilibrium state. After amino modification, the hydrophilic ability of NH_2-PAA/Alginate increases, and the swelling rate raised to 90%, while the hydrogel still maintains good mechanical property. Moreover, the metal ions have faster diffusion rate in the hydrogel with the higher water content [29]. The result of the zero charge point experiment is shown in Fig. 3d. The zero charge point of NH_2-PAA/Alginate is 8.2, higher than that of PAA/Alginate (zero charge point is 5.2), which is due to the introduction of amine groups.

3.2. Effect of environmental conditions

In order to investigate the influence of environmental conditions on the adsorption process, the adsorption experiments of Cd(II) on NH_2-PAA/Alginate under different pH, different ion species (Na, Mg, Ca) and ionic strength were studied. The pH of bulk solution precipitation (pH_{BSP}) for Cd(II) with initial concentration of 50 mg/L was 8.51, and no precipitation occurred at pH below pH_{BSP}. As shown in Fig. 4, the adsorption capacity of Cd(II) onto NH_2-PAA/Alginate at pH 1.5 could be negligible. The adsorption capacity sharply increased with increasing pH at range of 2~3.5, and finally retained about 48% at pH above 4. Generally, the solution pH is lower than the zero charge point (the value of NH_2-PAA/Alginate is 8.2), the surface of adsorption is positively charged for the protonation reaction, which is unfavorable for adsorption process due to the electrostatic repulsion towards positively charged metal ions [30]. while, the adsorption capacity of NH_2-PAA/Alginate could reach to adsorption saturation at pH above 4, indicating that the adsorption process of Cd(II) on NH_2-PAA/Alginate was dominated by chemical adsorption rather than electrostatic interactions [31]. In the range of pH 2.0 ~ 3.5, the protonation reaction will compete

with the heavy metal ion adsorption, and the adsorption process can be described as a liquid-solid interface ion exchange process [32]:

$$n\overline{SurH} + Cd(II) \Leftrightarrow \overline{Sur_nCd(II)} + nH^+ \qquad (4)$$

According to the thermodynamic equilibrium constant and distribution coefficient, the following relation can be deduced:

$$\log K_d = \log K_{eq} + n\log\left[\overline{SurH}\right] + npH \qquad (5)$$

where Sur is the surface of NH_2-PAA/Alginate, the overline labels refer to species on NH_2-PAA/Alginate, K_{eq} is the thermodynamic equilibrium constant. The logK_d *vs*. pH was plotted in Fig. 4c. The slope of the linear plot is close to 1, suggesting that the adsorption process involved with the exchange of one protons to aqueous phase when forming one Cd(II) complex. In fact, the Cd(II) also exchanges Ca(II) in NH_2-PAA/Alginate in the adsorption process, which could be illustrated from the analysis of the elements in XPS before and after gel adsorption (Table 1).

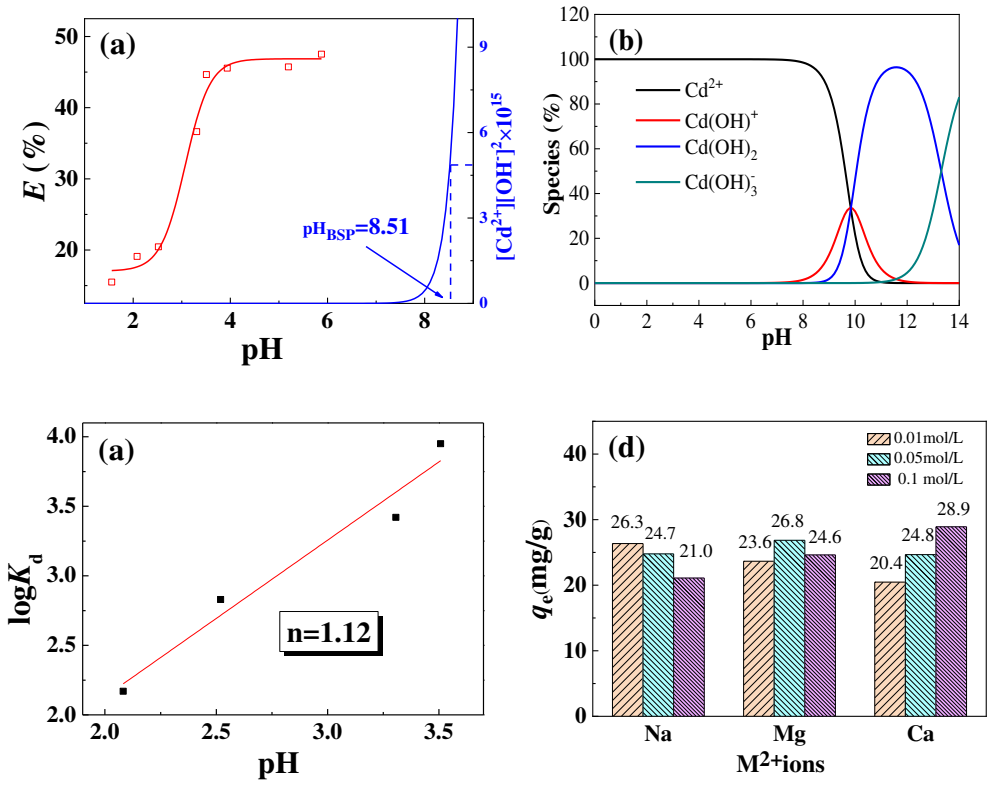

Fig. 4 (a) Effect of pH on Cd(II) adsorption by NH_2-PAA/Alginate (C_0 = 50 mg/L, t =4h, T = 298

K). (b) Distribution of radionuclide species in aqueous solutions. (c) Linear plot of logK_d and pH. (d) Effect of ion species and ionic strength on adsorption for Cd(II) (C_0 = 50 mg/L, t = 4h, T = 298 K, pH = 6.0).

Alkali metal and alkaline-earth metal ions are usually abundantly present in the actual industrial effluent. Although these ions are nontoxic and harmless, the competition adsorption between these ions and Cd(II) was observed. Fig. 4d shows the effects of Na(I), Mg(II) and Ca(II) on Cd(II) uptake by NH_2-PAA/Alginate. It can be seen that all ions in solution had small effect on Cd(II) adsorption. The increasing the concentration of Na(I), the adsorption efficiency of Cd(II) decreased, which could mainly cause by the electrostatic repulsion [33]. While the uptake of Cd(II) increase when increasing of Mg(II) and Ca(II) concentration, this phenomena could be illustrated the formation of ionic atmosphere at higher ion concentration and reduced impact on Cd(II) adsorption.

3.3. Adsorption kinetics

Adsorption kinetics is important in the prediction of the adsorption rate, which is highly demanded for adsorbents in practical application. The effect of time on the Cd(II) adsorption by the NH_2-PAA/Alginate is presented in Fig. 5. The adsorption of Cd(II) on the NH_2-PAA/Alginate increased rapidly within 100 min and reached adsorption equilibrium in approximately 150 min. For bulk material-based adsorbent, the adsorption rate is faster than that of most common granular adsorbents. Obviously, the fast adsorption rate of NH_2-PAA/Alginate should owe to the three-dimensional network, porous structure and its excellent water penetration which is highly accessible to Cd(II) [34].

In order to analyze the adsorption rate of Cd(II) on NH_2-PAA/Alginate, the pseudo-first-order, pseudo-second-order model and intraparticle diffusion model were employed to fit the experimental data. The fitted kinetic curves are shown in Fig. 5, and the fitted kinetic parameters are summarized in Table 2. The fitting results show that the correlation coefficients were 0.9383 for pseudo-first-order and 0.9539 for pseudo-

second-order, respectively. Obviously, the pseudo-second-order model gave the more significant goodness-of-fit, implying that the rate-limiting step could involve the chemical adsorption.

Generally, the adsorption process follows three steps of external diffusion, intraparticle diffusion and adsorption before reaching equilibrium. To understand the dominating step of adsorption, the intraparticle diffusion model could be employed to describe adsorption process. Two set of line segments were observed in the intraparticle diffusion model curves. According to this model, if intraparticle diffusion is the rate-controlling step, the first line with larger slope should pass through the origin [35]. While the above results are not in accord with the experiments, revealing that intraparticle diffusion was not the rate-limiting step whereas all the steps functioned simultaneously.

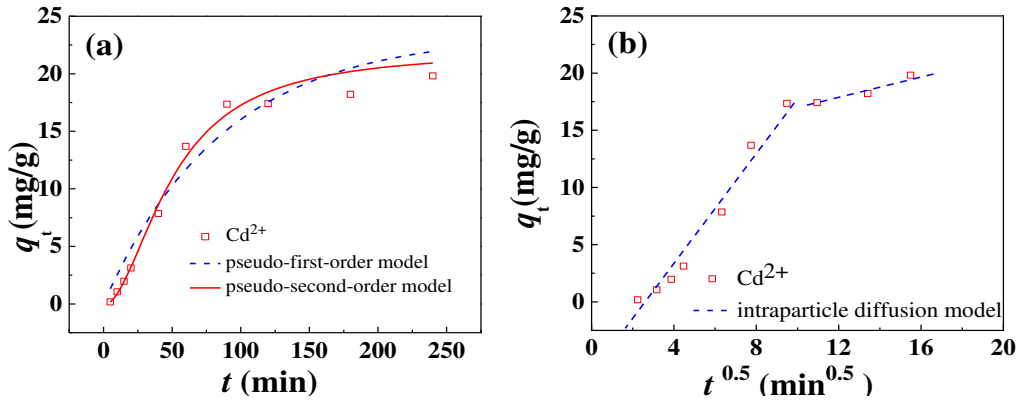

Fig. 5 Time-dependent Cd(II) sorption on hydrogel, the data are fittings to the Pseudo-first-order, Pseudo-second-order models and intraparticle diffusion model (C_0=50 mg/L, T = 25°C, pH = 6.0).

Table 2 Constants for the kinetic sorption data using different sorption models.

Dynamic adsorption model	Adsorbent kinetic parameter		
	K	q_e	R^2
First order kinetic model	0.013	21.05	0.9383
Second order kinetic model	0.000371	29.19	0.9539

3.4. Adsorption isotherms

The adsorption capacity of an adsorbent is usually evaluated by isothermal adsorption experiment, The isothermal adsorption data of NH_2-PAA/Alginate with different concentrations of Cd(II) at 25℃ are shown in Fig. 6. Obviously, the adsorption capacity increased with increasing Cd(II) concentrations, and finally approached the adsorption equilibrium at about 130 mg/g. To further study on the adsorption behavior, the Langmuir, Freundlich, Temkin and Langmuir-Freundlich isotherms were used to describe the adsorption of Cd(II) on NH_2-PAA/Alginate. The fitting curve of four models are shown in Fig. 6a and b and the corresponding parameters are listed in Table 3. The fitting results show that the correlation coefficient (R^2=0.9808) for Langmuir-Freundlich model was higher than that for the other three models, indicating the Langmuir-Freundlich equation was suitable to describe the adsorption of Cd(II), and the adsorption process involved the physical adsorption and monolayer adsorption of Cd(II) on NH_2-PAA/Alginate [36], such as ion exchange adsorption and coordination adsorption.

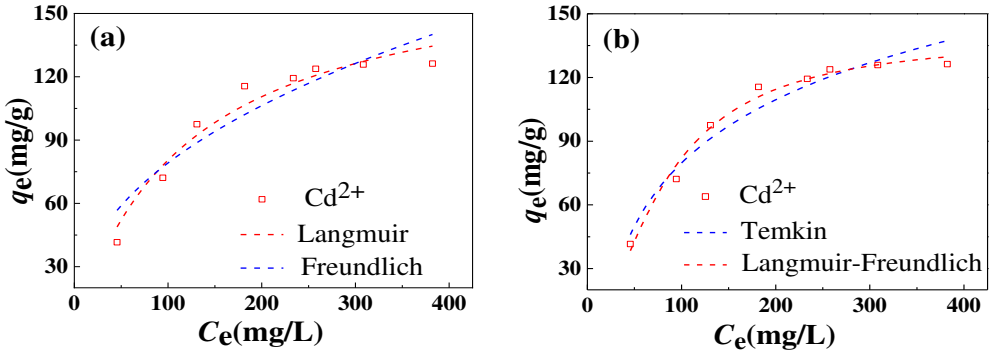

Fig. 6 The isothermal adsorption curves of Cd(II) by NH_2-PAA/Alginate (t = 4h, T = 298 K, pH = 6.0).

Table 3 Isotherm parameters of Cd(II) adsorption on the NH_2-PAA/Alginate.

Isotherms model	Parameter		
Langmuir	Q_{max}	K_L	R^2
	176.5	0.0083	0.9508
Freundlich	K_F	n	R^2
	11.16	2.351	0.8653

Temkin	b_r	A_r	R^2
	57.69	0.0641	0.9409
Langmuir- Freundlich	K_{LF}	n	R^2
	839.8	5925	0.9808

3.5. Selective adsorption and recyclability test

In the selective adsorption experiment, a mixed solution containing Cu(II), Cd(II), Pb(II), Zn(II), Mn(II), and Ni(II) with the same concentration as 50 mg/L was conducted. As shown in Fig. 7a, the Pb(II) was preferentially adsorbed with the adsorption efficiency of 79.8% by NH_2-PAA/Alginate. The adsorption efficiency of the other type of ions was in the order of Mn(II)>Cu(II)> Ni(II)> Cd(II)>Zn(II), within the range of 20% ~ 35%, indicating NH_2-PAA/Alginate has low selectivity while it can effectively treat the wastewater containing mixed heavy metal ions, such as the mining and smelting wastewater. Table 4 list the parameters of selective adsorption, the difference of K_d may be mainly caused by the difference of electronegativity (2.2 for Pb(II), 1.55 for Mn(II), 1.9 for Cu(II), 1.91 for Ni(II), 1.69 for Cd(II) and 1.65 for Zn(II)) [22], in addition, the mass-to-charge ratio, stability constant, chemical speciation, size of hydrated, and chelation ability of these bivalent heavy metal ions also lead to the difference of adsorption capacity [9].

The regeneration ability of adsorbents is one of the important indexes as it is closely related to the economy of water treatment technology. The result of influence of pH experiment indicating that the adsorption-desorption of Cd(II) on NH_2-PAA/Alginate could be facilely achieved by adjusting solution pH. Fig. 7b shows that the desorption efficiency of Cd(II) is high in the 0.1 M HCl solution, and the adsorption/ desorption performance of NH_2-PAA/Alginate maintained highly stable in each cycle. For example, the adsorption rate of the first cycle was 52.2%, while the adsorption rate of the fifth cycle decreased slightly to 48.2%. Obviously, the excellent recyclability of NH_2-PAA/Alginate could be attributed to its three-dimensional porous structure with

good mechanical stability.

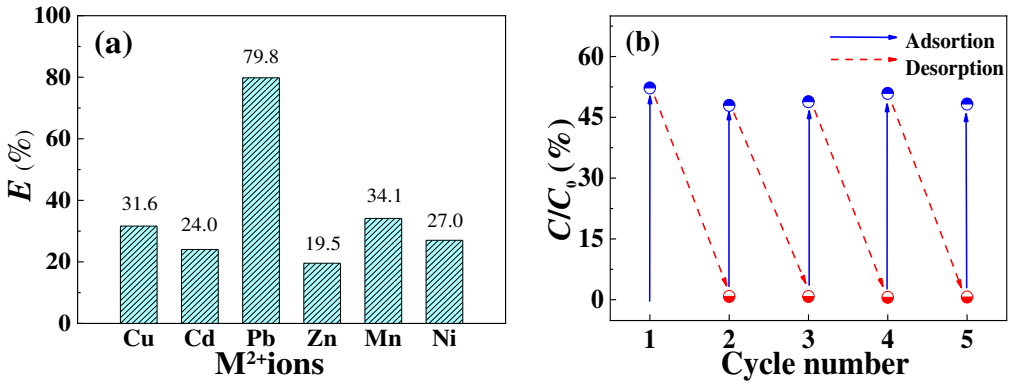

Fig. 7 (a) Selective adsorption of the NH_2-PAA/Alginate hydrogel in a mixed solution (C_0 = 50 mg/L, t = 4h, T = 298 K, pH = 6.0). (b) Recycling of NH_2-PAA/Alginate hydrogel in the removal of Cd(II) (C_0 = 50 mg/L, t = 4h, T = 298 K, pH = 6.0).

Table 4 The distribution adsorption coefficient of the five mixed ions

Ions	q_e/(g/g)	E/%	K_d/(L/g)	Electronegativity
Pb(II)	39.91	79.82	3.96	2.2
Mn(II)	17.07	34.13	0.52	1.55
Cu(II)	15.82	31.63	0.46	1.9
Ni(II)	13.51	27.02	0.37	1.91
Cd(II)	12.02	24.04	0.32	1.69
Zn(II)	9.78	19.56	0.24	1.65

3.6. Adsorption mechanism

The adsorption mechanism between adsorbent and heavy metal ions plays an important role for adsorption design. In the previous discussion, a preliminarily conclusion could be inferred that the Cd(II) adsorption by NH_2-PAA/Alginate was dominated by ion exchange and chemical adsorption. To further explore the adsorption mechanism, the XPS was used to analyze the chemical state of element in NH_2-PAA/Alginate and Cd-NH_2-PAA/Alginate. The XPS survey scan spectra (Fig. 8a) show photoelectron lines at binding energies of about 284, 347, 399 and 531 eV attributed to C1s, Ca2p, N1s and O1s, respectively. The characteristic peaks of $Cd3d_{5/2}$ and $Cd3d_{3/2}$

at 405 and 410 eV appeared obvious in Cd-NH_2-PAA/Alginate, while the characteristic peak of Ca2p became weaker, indicating that the part of Ca(II) was replaced by Cd(II) in the adsorption process [37]. This result also can be inferred by XPS element analysis in Table 1, the content of Ca elements decreased from 1.6% to 0.7%, while the content of Cd increased to 1.16%.

The high-resolution XPS spectra show that the binding energies of N1s had significant changed before and after adsorbing Cd(II) (Fig. 8c). There is mainly one typical N1s peak at 399.75 eV in –NH_2 groups of NH_2-PAA/Alginate, while after the adsorption of Cd(II), the characteristic peak shifted to higher positions at 400.56 eV, which indicates the formation of coordination bond between amino group and Cd(II). This can be interpreted that the Cd atom is able to accept isolated electron pair at N atom to form new compounds, and reducing the electron densities of the N atom [38]. In the high-resolution XPS spectra of O1s (Fig. 8d), there was slight shift of O1s peaks in Cd-NH_2-PAA/Alginate, and the integral area ratio of the two peaks of O1s at 532.5 eV (C=O) and 531.2 eV (C-O) for NH_2-PAA/Alginate and Cd-NH_2-PAA/Alginate increased from 0.430 to 0.491. indicating that the binding of Cd(II) also occurred at O atoms of hydroxyl group [27]. The results reveal that the Cd(II) exchanged with Ca(II) and then coordinated with amino and hydroxyl groups in NH_2-PAA/Alginate.

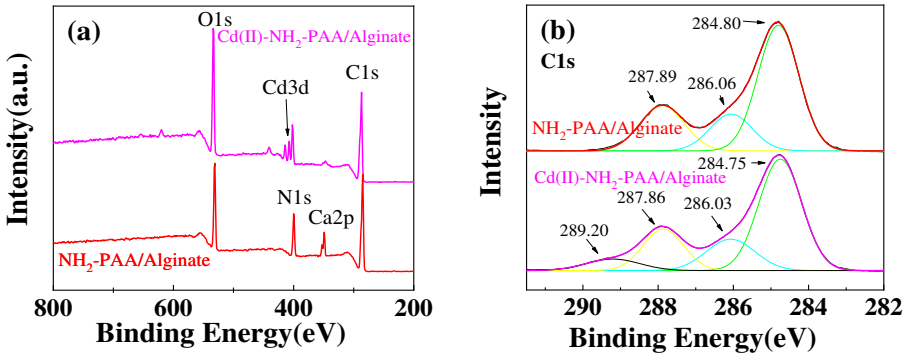

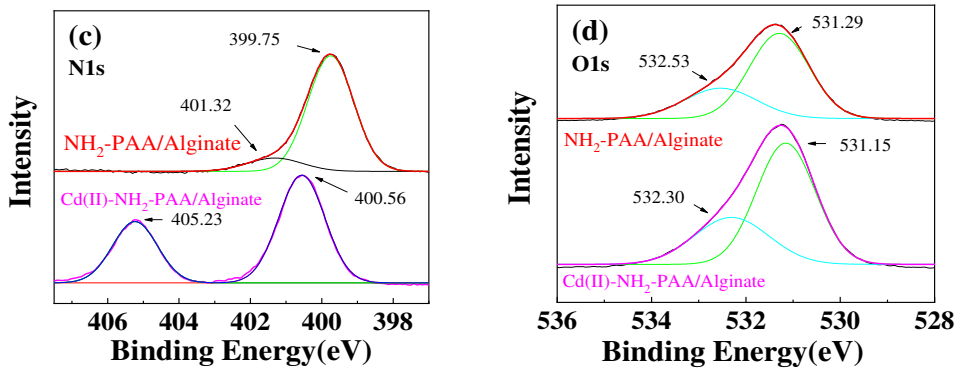

Fig. 8 The XPS spectra of NH_2-PAA/Alginate hydrogel, (a) total survey scan of XPS spectra; high-resolution XPS spectra of (b) C1s; (c) N1s; (d) O1s.

4 Conclusions

In this study, a new hydrogel with double network interpenetrating structure was well designed and prepared via simple radical polymerization and amino modification. The moisture of NH_2-PAA/Alginate was 90%, while the it exhibited the good mechanical strength. The Cd(II) adsorption on NH_2-PAA/Alginate was strongly dependent on pH and weakly dependent on ionic strength. The adsorption capacities were as high as 176.5 mg/g for Cd(II), and the equilibrium reached in 150 min. Besides, NH_2-PAA/Alginate had excellent adsorption capacity for various heavy metal ions in a mixed solution, and can be used to effectively treat mining and smelting industrial wastewater. In addition, the NH_2-PAA/Alginate could be easily regenerated and highly reused. The result of adsorption mechanism analysis illustrated that amino and hydroxyl groups in NH_2-PAA/Alginate involve in the adsorption process by chemical coordination with Cd(II). This wok opens a new window to develop high performance sorbents for the removal heavy metal ions. In summary, the NH_2-PAA/Alginate will be very suitable materials for the adsorption of heavy metal ions from large volumes of aqueous solutions in environmental pollution cleanup in the near future.

Acknowledgments

This work was supported by the National Natural Science Foundation of China [52070078, 51708204, 51774128], Hunan Provincial Natural Science Foundation of China [2018JJ3125, 2018JJ4009 and 2019JJ50137], and Scientific Research Project of

the Education Department of Hunan Province [19C0568, 17C0463].

References

1. S. Vasudevan, Int. J. Waste Resour. **6**, (2016).

2. A. M. Riederer, A. Belova, B. J. George, and P. T. Anastas, Environ. Sci. Technol. **47**, 1137 (2013).

3. K. Fu, X. Liu, D. Yu, J. Luo, Z. Wang, and J. C. Crittenden, Environ. Sci. Technol. **54**, 16212 (2020).

4. Q. Chen, W. Xu, and Q. Ge, Environ. Sci. Technol. **52**, 4464 (2018).

5. L. Ma, Q. Wang, S. M. Islam, Y. Liu, S. Ma, and M. G. Kanatzidis, J. Am. Chem. Soc. **138**, 2858 (2016).

6. H. Zhang, X. Quan, S. Chen, X. Fan, G. Wei, and H. Yu, Environ. Sci. Technol. **52**, 4827 (2018).

7. A. Martín-Domínguez, M. L. Rivera-Huerta, S. Pérez-Castrejón, S. E. Garrido-Hoyos, I. E. Villegas-Mendoza, S. L. Gelover-Santiago, P. Drogui, and G. Buelna, Sep. Purif. Technol. **200**, 266 (2018).

8. X. Du, S. Cui, X. Fang, Q. Wang, and G. Liu, J. Environ. Chem. Eng. **8**, 104530 (2020).

9. G. Zhou, J. Luo, C. Liu, L. Chu, and J. Crittenden, Water Res. **131**, 246 (2018).

10. Y. Kobayashi, F. Ogata, T. Nakamura, and N. Kawasaki, J. Environ. Chem. Eng. **8**, 103687 (2020).

11. J. Li, Q. Duan, Z. Wu, X. Li, K. Chen, G. Song, A. Alsaedi, T. Hayat, and C. Chen, Chem. Eng. J. **383**, 123189 (2020).

12. W. Cui, X. Zhang, C. I. Pearce, Y. Chen, S. Zhang, W. Liu, M. H. Engelhard, L. Kovarik, M. Zong, H. Zhang, E. D. Walter, Z. Zhu, S. M. Heald, M. P. Prange, J. J. De Yoreo, S. Zheng, Y. Zhang, S. B. Clark, P. Li, Z. Wang, and K. M. Rosso,

Environ. Sci. Technol. **53**, 11043 (2019).

13. S. Z. Mohammadi, Z. Safari, and N. Madady, J. Inorg. Organomet. Polym. Mater. **30**, 3199 (2020).

14. L. Huang, M. He, B. Chen, and B. Hu, Chemosphere **199**, 435 (2018).

15. I. Ali, Chem. Rev. **112**, 5073 (2012).

16. M. A. Haq, Y. Su, and D. Wang, Mater. Sci. Eng. C **70**, 842 (2017).

17. E. M. Ahmed, J. Adv. Res. **6**, 105 (2015).

18. J.-Y. Sun, X. Zhao, W. R. K. Illeperuma, O. Chaudhuri, K. H. Oh, D. J. Mooney, J. J. Vlassak, and Z. Suo, Nature **489**, 133 (2012).

19. S. De Koker, J. Cui, N. Vanparijs, L. Albertazzi, J. Grooten, F. Caruso, and B. G. De Geest, Angew. Chemie - Int. Ed. **55**, 1334 (2016).

20. Y. S. Zhang and A. Khademhosseini, Science (80-.). **356**, eaaf3627 (2017).

21. M. Khan and I. M. C. Lo, Water Res. **106**, 259 (2016).

22. J. Tang, J. Huang, G. Zhou, and S. Liu, J. Chem. Thermodyn. **141**, 105918 (2020).

23. Y. Tan, Y. Zhang, Y. Zhang, J. Zheng, H. Wu, Y. Chen, S. Xu, J. Yang, C. Liu, and Y. Zhang, Chem. Mater. **32**, 7670 (2020).

24. Y. Zhou, C. Wan, Y. Yang, H. Yang, S. Wang, Z. Dai, K. Ji, H. Jiang, X. Chen, and Y. Long, Adv. Funct. Mater. **29**, 1806220 (2019).

25. H. Wang, X. Hu, Y. Guo, C. Qiu, S. Long, D. Hao, X. Cai, W. Xu, Y. Wang, and Y. Liu, J. Chem. Technol. Biotechnol. **93**, 2447 (2018).

26. G. Zhou, C. Liu, L. Chu, Y. Tang, and S. Luo, Bioresour. Technol. **219**, 451 (2016).

27. Z. Ahmed, P. Wu, L. Jiang, J. Liu, Q. Ye, Q. Yang, and N. Zhu, Colloids Surfaces A Physicochem. Eng. Asp. **604**, 125285 (2020).

28. J. Shi, H. Zhang, Y. Yu, X. Zou, W. Zhou, J. Guo, Y. Ye, and Y. Zhao, J. Inorg. Organomet. Polym. Mater. **30**, 2114 (2020).

29. H. Li, H. Zheng, Y. J. Tan, S. B. Tor, and K. Zhou, ACS Appl. Mater. Interfaces **13**, 12814 (2021).

30. L. Chu, C. Liu, G. Zhou, R. Xu, Y. Tang, Z. Zeng, and S. Luo, J. Hazard. Mater. **300**, 153 (2015).

31. L. Gong, Y. Kong, H. Wu, Y. Ge, and Z. Li, J. Inorg. Organomet. Polym. Mater. **31**, 659 (2021).

32. M. Hasanpour and M. Hatami, Adv. Colloid Interface Sci. **284**, 102247 (2020).

33. R. Katiyar, A. K. Patel, T.-B. Nguyen, R. R. Singhania, C.-W. Chen, and C.-D. Dong, Bioresour. Technol. **328**, 124829 (2021).

34. Y. Yu, L. Shang, J. Guo, J. Wang, and Y. Zhao, Nat. Protoc. **13**, 2557 (2018).

35. A. Hashem, A. J. Fletcher, M. El-Sakhawy, L. A. Mohamed, and S. Farag, J. Polym. Environ. **28**, 2498 (2020).

36. L. Guan, H. Kang, W. Liu, and D. Tian, Int. J. Biol. Macromol. **177**, 48 (2021).

37. W. Zhang, X. He, G. Ye, R. Yi, and J. Chen, Environ. Sci. Technol. **48**, 6874 (2014).

38. G. Zhou, J. Luo, C. Liu, L. Chu, J. Ma, Y. Tang, Z. Zeng, and S. Luo, Water Res. **89**, 151 (2016).

Figures

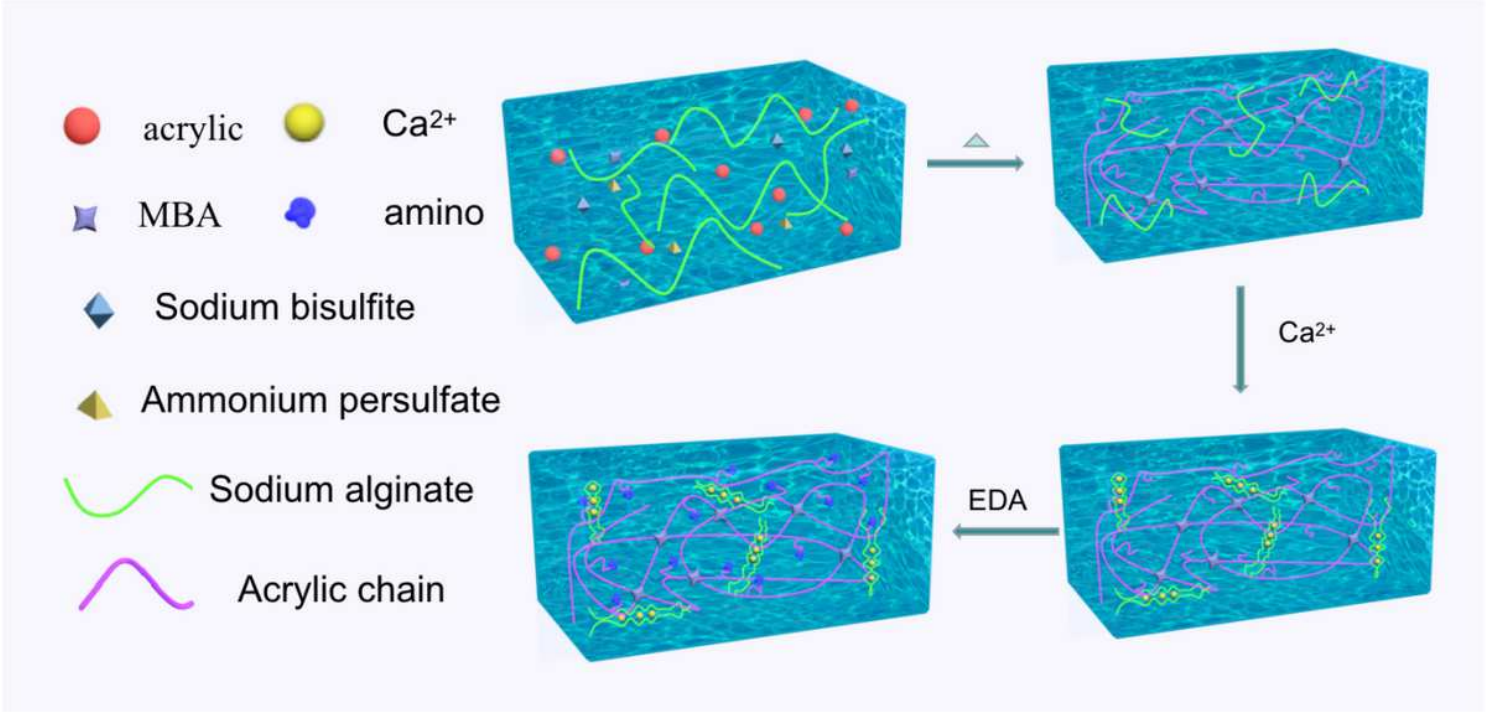

Figure 1

Mechanisms of converting the composite into NH2-PAA/Alginate DN hydrogels.

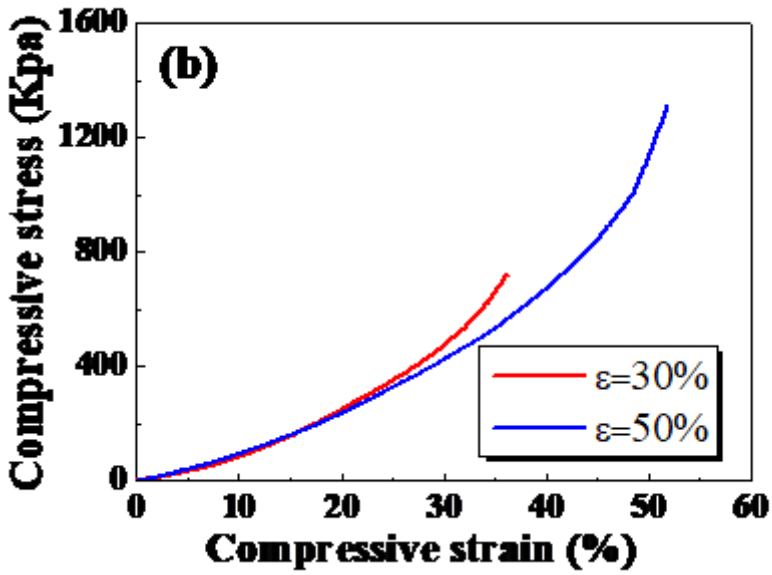

Figure 2

(a) The SEM image of NH2-PAA/Alginate. (b) Typical consecutive loading curves with gradually increased strain on NH2-PAA/Alginate.

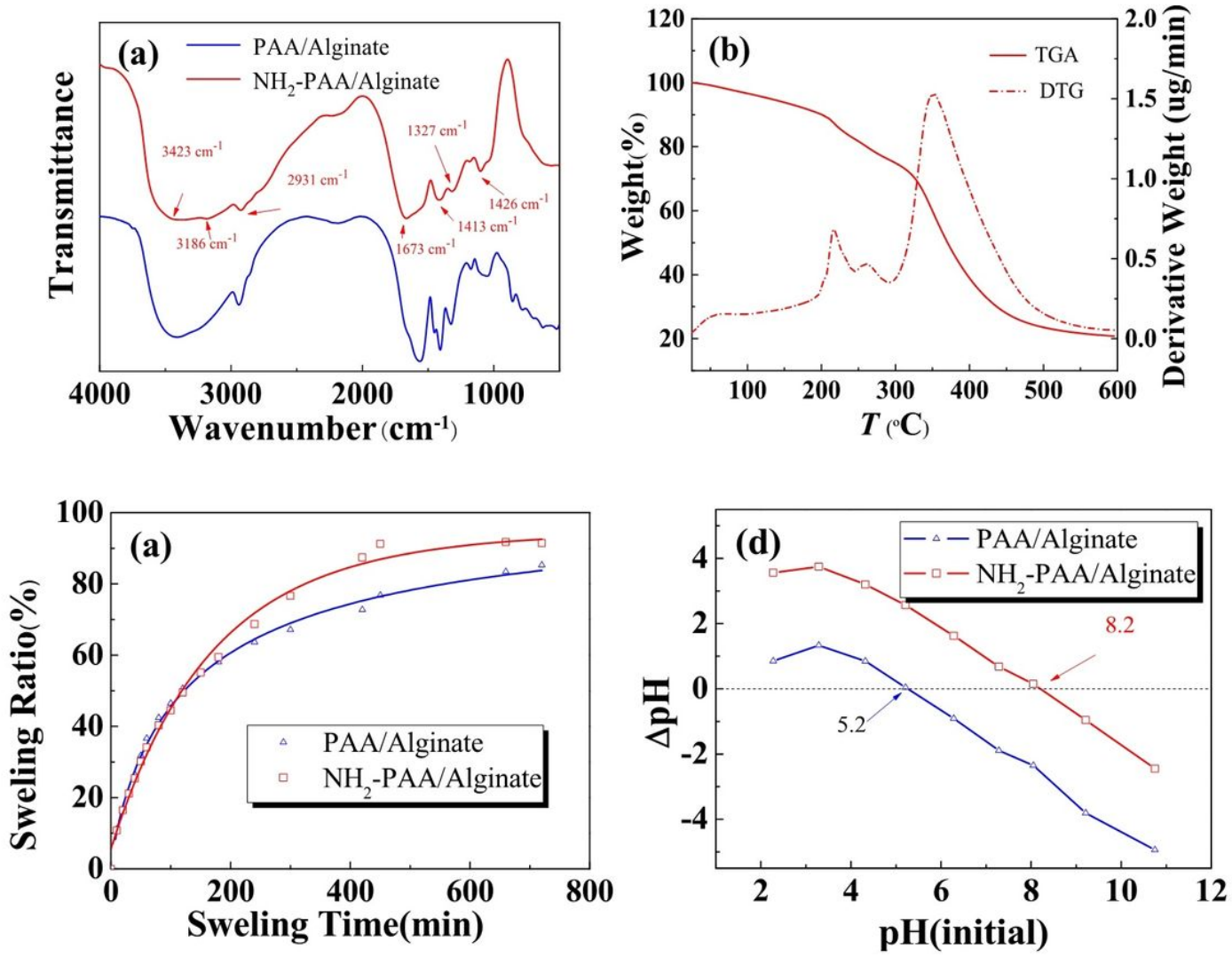

Figure 3

(a) The FTIR spectra. (b) The TGA and DTG curves. (c) The swelling curves. (d) The pHpzc measure of the hydrogel by ΔpH method.

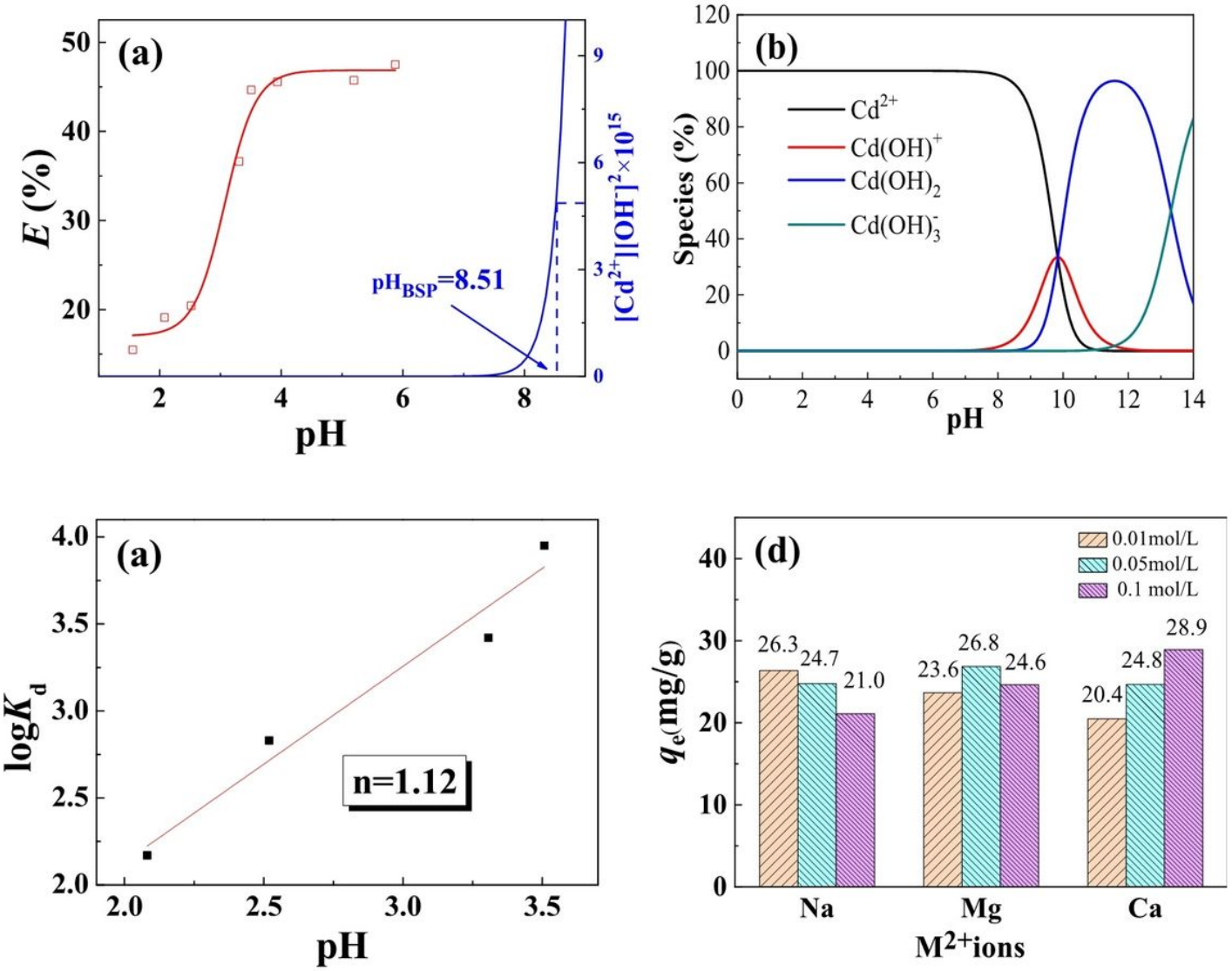

Figure 4

(a) Effect of pH on Cd(II) adsorption by NH2-PAA/Alginate (C0 = 50 mg/L, t =4h, T = 298 K). (b) Distribution of radionuclide species in aqueous solutions. (c) Linear plot of logKd and pH. (d) Effect of ion species and ionic strength on adsorption for Cd(II) (C0 = 50 mg/L, t = 4h, T = 298 K, pH = 6.0).

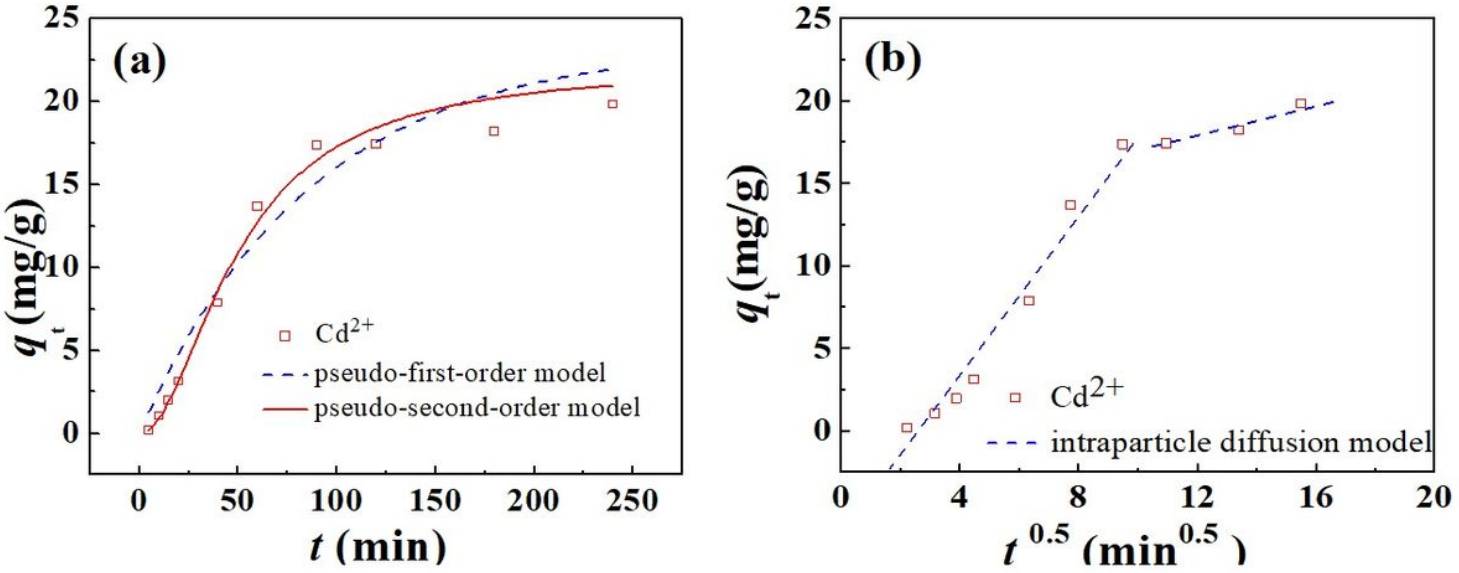

Figure 5

Time-dependent Cd(II) sorption on hydrogel, the data are fittings to the Pseudo-first-order, Pseudo-second-order models and intraparticle diffusion model (C0=50 mg/L, T = 25℃, pH = 6.0).

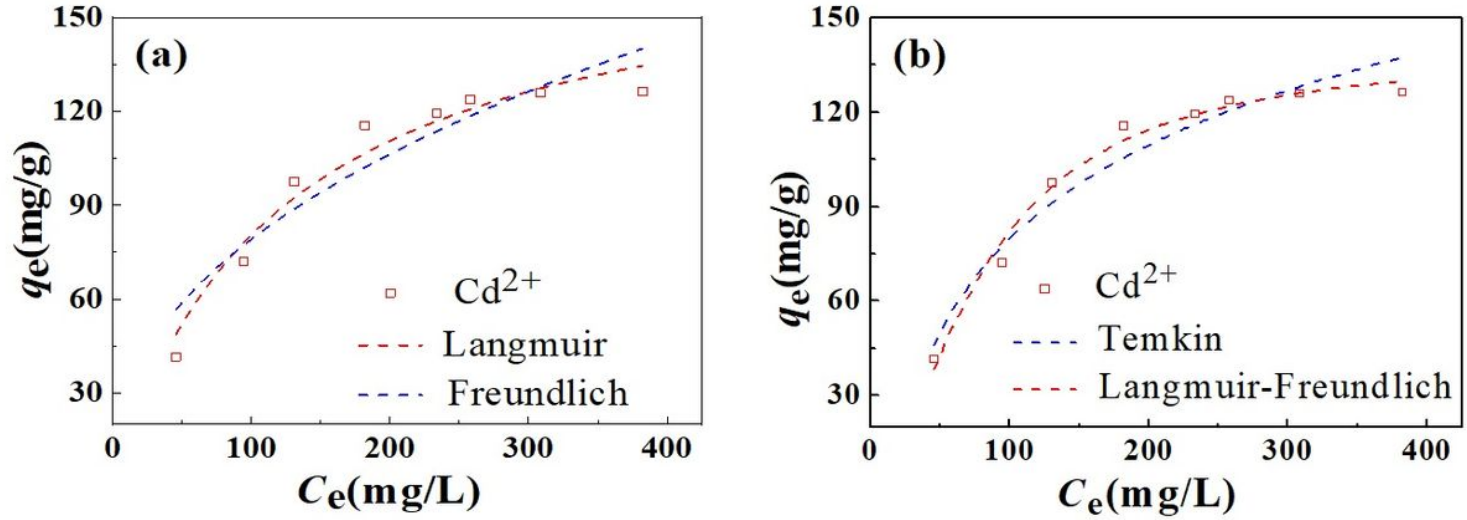

Figure 6

The isothermal adsorption curves of Cd(II) by NH2-PAA/Alginate (t = 4h, T = 298 K, pH = 6.0).

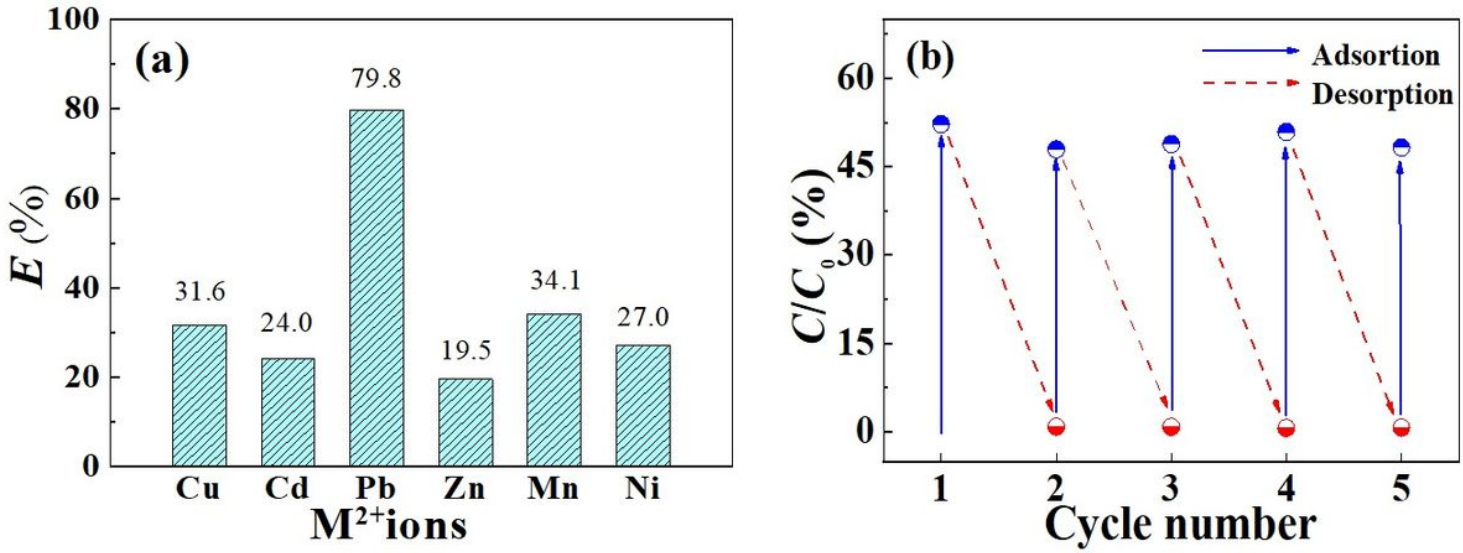

Figure 7

(a) Selective adsorption of the NH2-PAA/Alginate hydrogel in a mixed solution (C0 = 50 mg/L, t = 4h, T = 298 K, pH = 6.0). (b) Recycling of NH2-PAA/Alginate hydrogel in the removal of Cd(II) (C0 = 50 mg/L, t = 4h, T = 298 K, pH = 6.0).

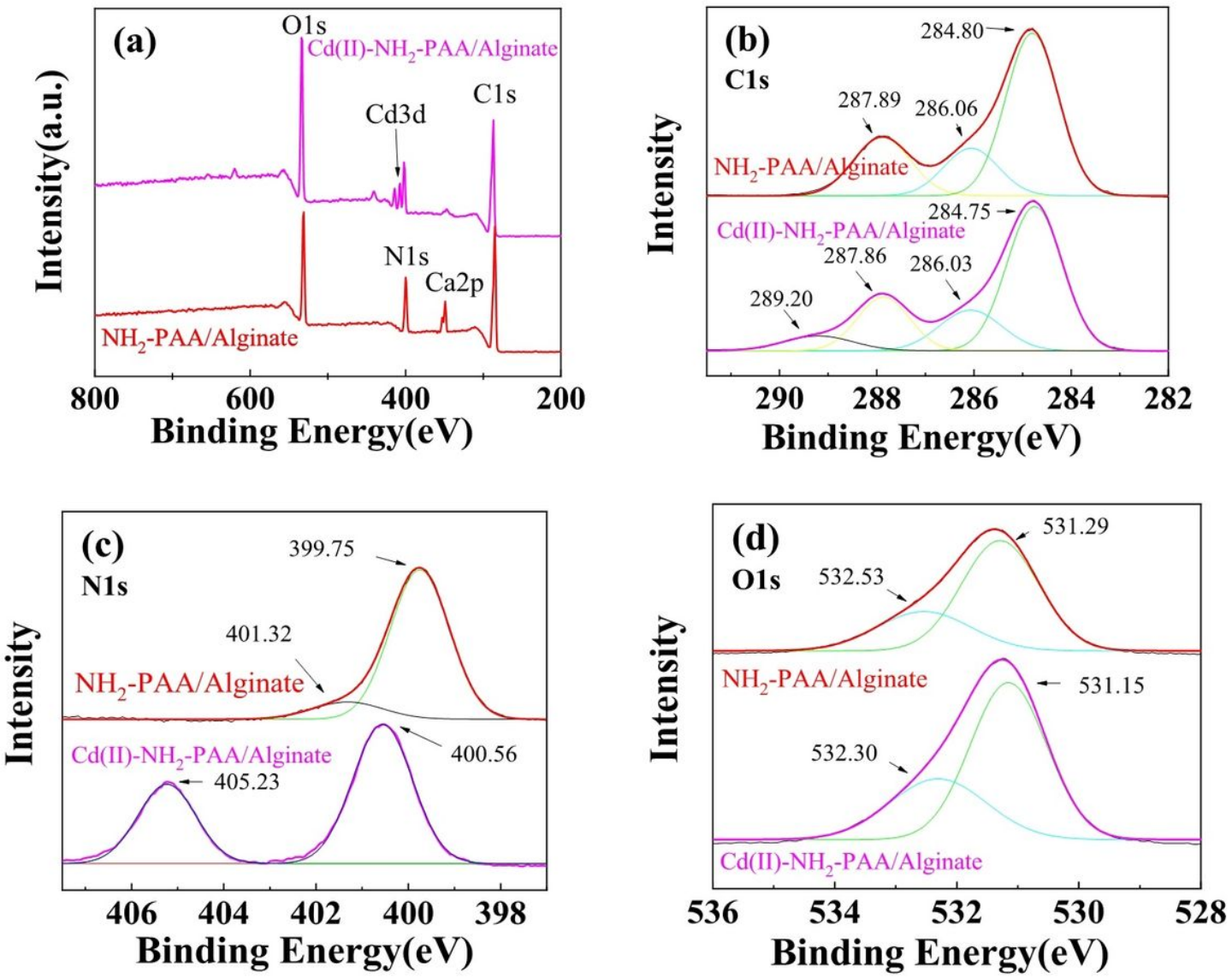

Figure 8

The XPS spectra of NH2-PAA/Alginate hydrogel, (a) total survey scan of XPS spectra; high-resolution XPS spectra of (b) C1s; (c) N1s; (d) O1s.